The effect of temporal fluctuations in r_0 on high-resolution observations

Robert N. Tubbs[a]

[a]Osservatorio Astrofisico di Arcetri, Largo E.Fermi, 5. 50125 Firenze, Italy

ABSTRACT

Previous experimental measurements and theoretical modelling indicate that atmospheric turbulence is expected to show intermittency (or "clumpiness"). The impact that this intermittency has on simulated adaptive optics (AO) and Lucky Imaging (LI) performance is assessed in this SPIE contribution using simulated phase screens with Von Karman power spectra which incorporate turbulent intermittency. The statistics of the intermittency model used are based as closely as possible on astronomical seeing measurements at real observatories. The performance of realistic AO correction of large Taylor screens with intermittent turbulence is compared directly with the performance given with traditional Gaussian random Taylor screens having the same Von Karman power spectrum. Also discussed is the improvement in performance which can be obtained by modifying the AO control parameters in response to the changing seeing conditions. Lucky Imaging simulations indicate that the performance of this method can be significantly improved under intermittent seeing.

Keywords: adaptive optics, simulation, astronomical seeing, intermittent seeing

1. INTRODUCTION

Both laboratory experiments[1] and astronomical seeing monitor measurements[2–5] have shown that atmospheric seeing conditions vary with time with a wide range of timescales. In the fluid dynamics community, fluctuations in the level of turbulence are called *turbulent intermittency* and are seen even in experiments with unchanging external flow conditions, sometimes exhibiting a quasi-periodic nature. In the case of astronomical seeing, variations in external inputs (such as solar heating) may contribute further to the variations seen in the atmospheric turbulence. In some cases it is necessary to model these fluctuations in astronomical seeing conditions in order to realistically simulate the performance of astronomical instruments.

Many of the parameters describing current adaptive optics (AO) systems can be varied in response to changing observing conditions. This is particularly important in AO systems which utilise non-linear wavefront sensors where, for the example of a pyramid sensor, the amplitude of the tip-tilt modulation is generally varied with the seeing conditions so that the residual phase across the pupil does not saturate the wavefront sensor.

In this article I describe an approach for simulating variations in seeing, thus allowing direct measurements of the benefit obtained from varying the parameters governing the AO system in a controlled simulation environment. Simple examples of the use of these intermittent turbulence simulations are presented, including the case of a simple AO system with pyramid wavefront sensor and Zernike mode correction, and the case of Lucky Imaging (LI).

Further author information: (Send correspondence to R.N.T.)
R.N.T.: E-mail: rtubbs@arcetri.astro.it, Telephone: +390552752202

2. MEASUREMENTS OF TURBULENT INTERMITTENCY

Studies of the temporal fluctuations in seeing using seeing monitors located at astronomical observatories have generally found that temporal decorrelation of the measured seeing typically occurs over timescales of 40-75 minutes,[2,4,5] with the temporal autocorrelation of seeing measurements being well-described by an exponential for time differences of many minutes or hours. High temporal resolution measurements[3] hint that that this law may break down at the very shortest timescales (a few minutes or less), and there is anecdotal evidence of substantial changes in seeing (up to a factor of 2) occurring on extremely short timescales (sometimes less than a second).[6,7]

Laboratory experiments have found intermittency in turbulent flow on short timescales (see e.g. Ref. 1). Unfortunately there appears to be some disagreement as to the best approach for theoretical modelling of this intermittency.[8–12]

The lack of a single preferred model for turbulent intermittency has pushed the studies of turbulent intermittency presented here towards a general formalism which can be modified to fit a range of different models for intermittency.

3. MODELS OF TURBULENCE

The conventional Gaussian random model for a phase screen with Kolmogorov (or Von Karman) turbulence[13] with no intermittency is usually generated in the following way:

$$\phi(\mathbf{r}) = Re\left(FT\left(R(\mathbf{k})\,K(\mathbf{k})\right)\right) \tag{1}$$

where $R(\mathbf{k})$ is a 2 dimensional square array of independent random complex numbers which have a Gaussian distribution about zero and white noise spectrum, $K(\mathbf{k})$ is the (real) Fourier amplitude expected from the Kolmogorov (or Von Karman) spectrum, $Re()$ represents taking the real part, and $FT()$ represents a discrete Fourier transform of the resulting 2 dimensional square array (typically an FFT).

This is the special case which generates Gaussian random phase fluctuations. A more general form which includes intermittency is:

$$\phi(\mathbf{r}) = Re\left(FT\left(\left[R(\mathbf{k}) \otimes I(\mathbf{k})\right]K(\mathbf{k})\right)\right) \tag{2}$$

where $I(\mathbf{k})$ is a 2 dimensional array which represents the spectrum of intermittency, with the same dimensions as $R(\mathbf{k})$, and where $\otimes$ represents convolution. The intermittency is described in terms of fluctuations in the turbulence strength[13] C_N^2. It can be seen that Equation 1 is just the special case from Equation 2 with:

$$I(\mathbf{k}) = \delta(|\mathbf{k}|) \tag{3}$$

where $\delta()$ is the Dirac delta function.

Note that whatever form $I(\mathbf{k})$ takes, $[R(\mathbf{k}) \otimes I(\mathbf{k})]$ will always keep its flat spectrum (as a function of $\mathbf{k}$), as long as $I(\mathbf{k})$ is not correlated to the random number array $R(\mathbf{k})$. This means that in practice the Kolmogorov (or Von Karman) amplitude spectrum (described by $K(\mathbf{k})$) is always preserved by Equation 2 whatever the form of the intermittency spectrum $I(\mathbf{k})$.

The statistics of all physically realistic, isotropic intermittent turbulence screens can be described by the real array $K(\mathbf{k})$ (describing the amplitude spectrum of the fluctuations) and the complex array $I(\mathbf{k})$ describing the intermittency of the turbulence.

4. SIMULATION METHOD

It is clear that real astronomical seeing does vary with position and time on the very largest scales, so that $I(\mathbf{k})$ is certainly not the delta function implied by Equation 1, but it remains to be seen what the experimentally determined form of this function will be. As a first approximation, I will assume that the expected value of the *intermittency* is the same at all locations in real space. This implies that $I(\mathbf{k})$ will have a Gaussian random form with its statistical properties fully described as an expected amplitude at each spectral frequency (with a random phase at each spectral frequency). The shape of this power spectrum could potentially be measured experimentally. For the case of a wind-blown Taylor screen, $|I(\mathbf{k})|^2$ is simply the Fourier transform of the temporal autocorrelation of the turbulence strength, which many authors[2,4] fit with an exponential.

It is well known that the intensity of atmospheric seeing varies with time. To keep the simulations as simple as possible, I have chosen to describe the atmosphere as a series of thin wind-blown Taylor screens. If the seeing was correctly described by a fixed Taylor screen, this would imply variations in seeing with position within the Taylor screen. In this way the temporal variations in turbulence are converted into spatial turbulence variations in a wind-blown screen. This approach has the benefit that it naturally includes one or more wind velocities within the simulated turbulence.

In order to make the Taylor screens decorrelate as they cross the telescope aperture, the Taylor screens I use here are modelled with Markov boiling, using a similar method to that described by Glindemann et al.[14] The boiling process is applied to the 2-dimensional array of random numbers ($R(\mathbf{k})$ in Equation 2). Note that the weightings of the changes to the Fourier components must be slightly different to those described in Ref. 14 as here $R(\mathbf{k})$ has a white-noise spectrum, while in Ref. 14 the random number array has already been filtered with the Kolmogorov amplitude spectrum. Note also that in our case the filtering with the Kolmogorov or Von Karman amplitude spectrum $K(\mathbf{k})$ *must* occur later to prevent this amplitude spectrum from being corrupted through convolution with the intermittency function $I(\mathbf{k})$.

Once the spectrum of the turbulent intermittency $I(\mathbf{k})$ has been defined, it is best to Fourier transform it to form a real space description of the intermittency. The algorithm for applying Markov boiling and turbulent intermittency is summarised in Figure 1. If the turbulent boiling is to be a Markov process with the correct temporal power spectrum, it is essential that the real space arrays describing the turbulent intermittency screens are shifted in space with the same wind velocities as the corresponding phase screens. The phase screen and intermittency screen arrays should be rotated on a "conveyor belt", as explained in Figure 2, keeping to the periodic boundary conditions of the discrete Fourier transform.[15] This conveyor belt shift of the screen only applies phase changes to the components of the discrete Fourier transform of the screen without affecting the Fourier amplitude (in fact to speed up computation, the wind shift can be applied in the Fourier domain, thus reducing the total number of Fourier transform operations by one).

The algorithm described in Figure 1 is very similar to that used by Glindemann et al,[14] but here the random number array has a white noise spectrum rather than a Kolmogorov amplitude spectrum. When the Taylor screen random number array is multiplied by the Fourier transform of the intermittency spectrum, intermittent white noise is produced (note that the flat spectrum of the noise is never affected by the introduction of intermittency, except for the unrealistic case of intermittency which is directly correlated with the random white noise).

The intermittent white noise output from Figure 1 must then be filtered to give it a Kolmogorov or Von Karman spectrum. This process is described in Figure 3. The entire Taylor screen array must be Fourier transformed, and the result must be multiplied by the Kolmogorov or Von Karman amplitude spectrum. An additional discrete Fourier transform is then used to return the phase screen array with intermittent Kolmogorov or Von Karman turbulence.

The screens have a finite size, and are blown past on a repeating conveyor belt (as shown in Figure 2). However the Markov boiling process ensures that all but the lowest Fourier components have become fully decorrelated with each full rotation of the conveyor belt, so that only the tip-tilt contribution shows any significant correlation from one rotation of the conveyor belt to the next. The speed of decorrelation was based on the decorrelation of the phase observed in measurements of turbulence blown across the William Herschel Telescope.[16,17] In most cases long simulations can be run using turbulence generated in this fashion even though the conveyor belt Taylor

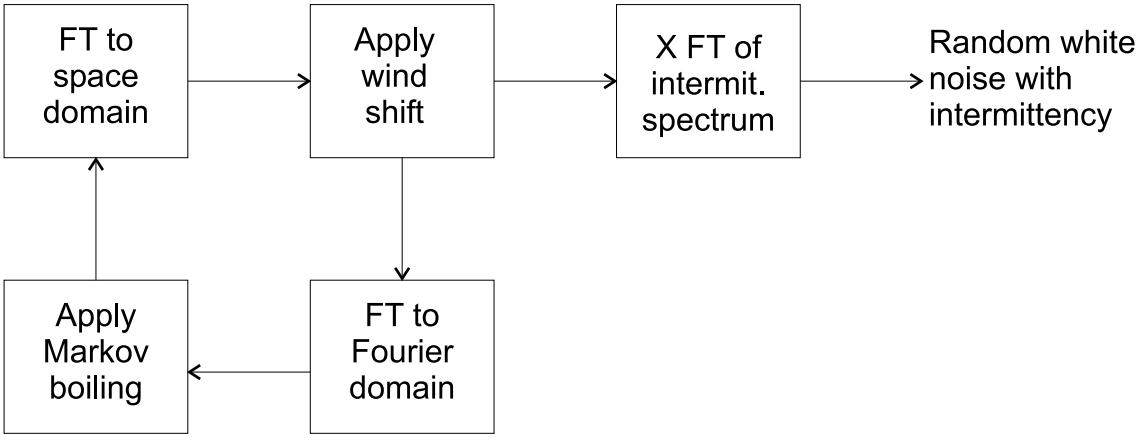

Figure 1. Markov boiling was applied to each wind-blown Taylor screen using a similar approach to Glindemann et al.[14] At this stage the Taylor screens contained random white noise – the Von Karman spectrum was applied at a later stage. At each time-step a copy of the Taylor screen was multiplied by the Fourier transform of the intermittency spectrum to give intermittent noise with a perfectly flat (white) spectrum. Note that the computation time can be reduced by applying the wind shift in the discrete Fourier domain, and only transforming to the time domain when applying the intermittency.

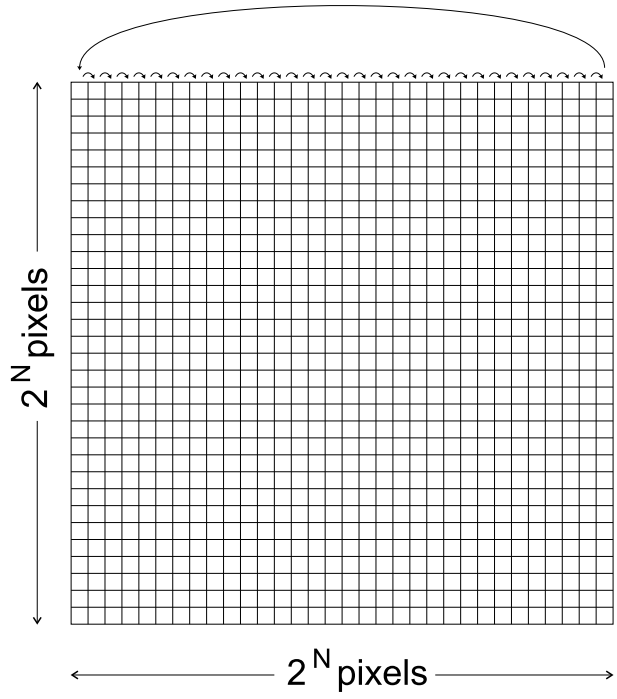

Figure 2. In the "conveyor belt" wind shift model, a screen is shifted sideways pixel by pixel. The data which shifts out of the right hand of the array is re-inserted back into the array on the left-hand side. The arrays are typically square with 2^N pixels on a side to allow efficient FFTs. This type of wind shift can also be applied in the Fourier domain using phase-rotation.

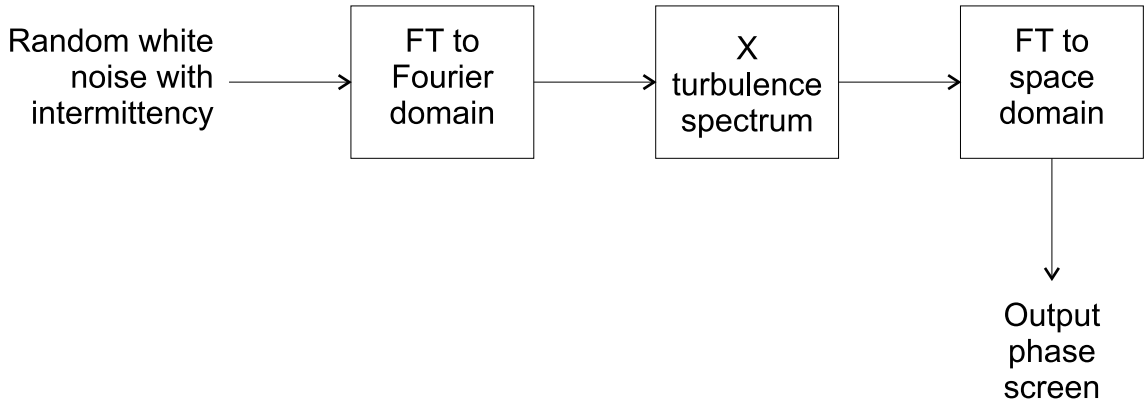

Figure 3. Application of the atmospheric amplitude spectrum to the intermittent random noise array.

screen has repeated itself several times. However, note that the intermittency pattern will repeat itself with each rotation of the conveyor belt.

5. SIMULATION RESULTS

Equation 2 ensures that the Fourier amplitude spectrum of the simulated phase screen is unaffected by the application of intermittency. This guarantees that the introduction of intermittency will not affect the Kolmogorov or Von Karman spectrum of the phase screens (which might make the simulations inconsistent with experimental measurements of astronomical seeing[18–21]). However, it is also important to check that the second-order structure function of the phase D_ϕ is unaffected, where D_ϕ is:

$$D_\phi(\rho) = \left\langle \left|\phi_a(\mathbf{r}) - \phi_a(\mathbf{r}+\rho)\right|^2 \right\rangle_{\mathbf{r}} \tag{4}$$

and ρ corresponds to a separation vector in the phase screen.

Simulations were performed both with and without turbulent intermittency, using a 4ms iteration timestep. Two models of intermittency were used, one with a Normal distribution of C_N^2 strength, and one with a log-Normal distribution of C_N^2 strength. Each simulation presented here involves two screens blown past the telescope with different wind velocities – corresponding to 10ms^{-1} and 18ms^{-1} at an 8m telescope (or 5ms^{-1} and 9ms^{-1} at a 4m telescope). The normalised turbulence strength averaged over a $20r_0$ diameter telescope pupil is plotted over the first 8 seconds of the simulation in Figure 4. Both intermittent turbulence models had an RMS variation of 16% about the mean of this pupil-averaged turbulence strength. The turbulence strength had an exponentially decaying temporal autocorrelation function, decorrelated over a timescale of 1.0s. Although this decorrelation time is much shorter than the timescales for fluctuations in seeing measured by seeing monitors with low temporal resolution,[2–5] this level of seeing fluctuation is not inconsistent with the rapid changes seen in high temporal resolution measurements.[6,7] The use of such a short autocorrelation timescale allows a wide variety of conditions to be explored in a short computer simulation. The same random number seed was used to generate the Markov Taylor screens in each model, so that the only difference between the final phase screens were the fluctuations in the turbulence strength.

The second-order structure function D_ϕ was calculated at 64 time-points distributed uniformly over 16 second simulations using each of the three intermittency models. The values of D_ϕ were averaged over all of these time points for each value of $|\rho|$. Plots of $D_\phi(|\rho|)$ for each model are shown in Figure 5. As expected the intermittency does not have a systematic effect on the measured structure function. This simulation method is thus able to generate phase fluctuations which mimic those expected from intermittent turbulence while retaining both the temporal and spatial power spectra observed in experiments and the second-order structure function expected for Kolmogorov turbulence.

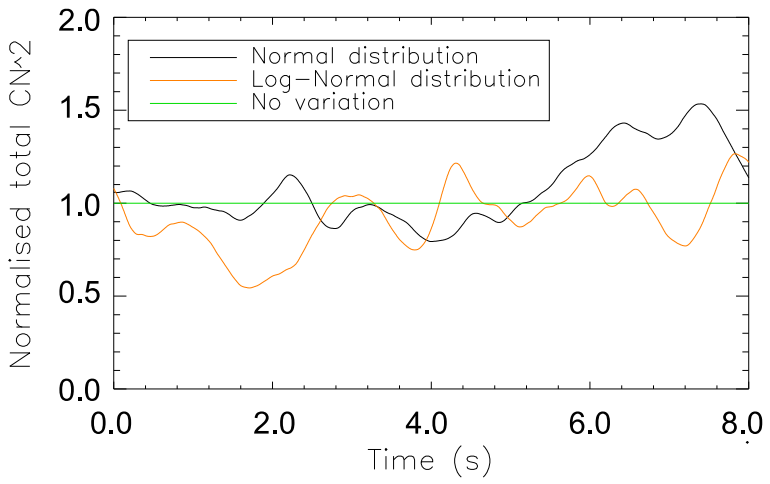

Figure 4. Normalised turbulence strength averaged over the telescope pupil for the three intermittency models described in the text is plotted against time for the first 8 seconds of each simulation.

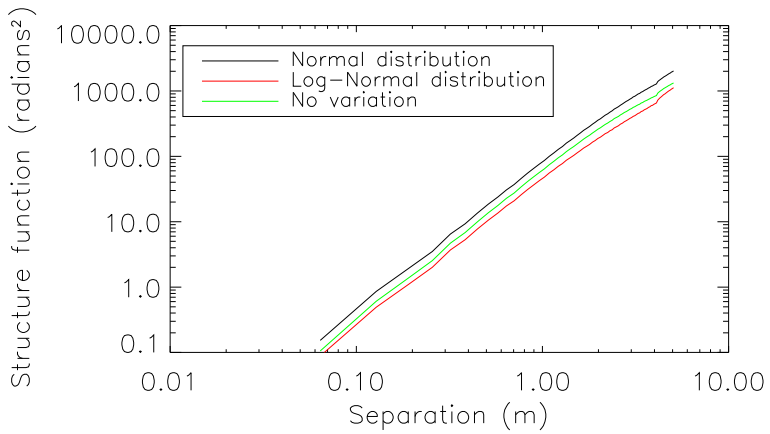

Figure 5. The second-order structure function D_ϕ calculated over separations $|\rho|$ much smaller than the outer scale, for three simulations with different types of intermittency. The same random number seed was used for generating the phase screens in all of the simulations, so the statistical noise on the three curves is correlated. The telescope diameter is 8m.

6. EFFECT OF TURBULENT INTERMITTENCY ON ADAPTIVE OPTICS CORRECTION

In order to investigate the effect of turbulent intermittency on adaptive optics correction, a series of simulations were undertaken using a deformable thin-shell mirror with pyramid wavefront sensor, similar to those performed for the Large Binocular Telescope.[22]

The AO simulations were developed in order to assess the effect of turbulent intermittency on the correction achieved, and to investigate approaches for optimising the AO performance under intermittent seeing conditions. The simulations utilised the correction of Zernike modes up to mode 104, based on measurements from a simulated pyramid wavefront sensor, (see e.g. Ref. 22). In the usual way, circular tip-tilt modulation was applied to the light beam before it reached the image plane pyramid, using a modulation period equal to the CCD exposure time. D/r_0 is 20 at the wavefront sensor wavelength for the AO simulations.

6.1. Preliminary simulations

In order to characterise the properties of the AO system, preliminary simulations were performed to investigate the dependence of the AO performance on the combined influences of the turbulence strength and the amplitude of the tip-tilt modulation. In these preliminary simulations, the Fourier spectrum of the intermittency $I(\mathbf{k})$ had power at only one frequency – the intermittency was the Fourier transform of a sinusoid with modulation in the direction of the wind velocity. This provided a 0.25Hz sinusoidal variation in the turbulence strength, which was ideal for characterising the AO performance under a variety of seeing conditions.

Simulations were performed with a range of different tip-tilt modulation amplitudes, in order to find which modulation amplitude provided the best correction under each set of seeing conditions. The phase residuals measured in the telescope pupil as a function of time are shown in Figure 6 for the first 16 seconds of each simulation – the 0.25Hz sinusoidal variation in the turbulence strength is clear. The modulation amplitude which provided the best correction during good seeing conditions gave the worst correction during poorer seeing conditions, and vice-versa. The modulation amplitude which provided the best correction was then plotted against the RMS measured wavefront sensor residual, and a best fit line was calculated. This line gave a way of estimating the optimum tip-tilt modulation to use for a given level of measured wavefront sensor residuals. A further simulation was then performed using varying tip-tilt modulation amplitude, switching the interaction matrix and bias levels whenever the modulation amplitude was changed. The best fit line of optimum modulation amplitude against wavefront sensor residuals was used to estimate the best tip-tilt modulation at each point in the simulation. The phase residuals measured in the telescope pupil for this simulation are plotted in a darker shade in Figure 6 – at almost all time points the simulation with varying AO correction is equal to or better than that provided by simulations which had fixed modulation amplitude.

6.2. Simulations with random intermittency

In order to test the AO correction with slightly more realistic intermittency, the simulations with random intermittency shown previously in Figure 4 were repeated using the two types of AO correction:

1. AO correction with a fixed modulation amplitude, which was chosen so as to be large enough to avoid saturating the detector even during the worst seeing conditions
2. AO correction with varying modulation amplitude, determined by the RMS signal measured on the wavefront sensor

With no turbulent intermittency (a classical atmospheric simulation), variation of the tip-tilt modulation amplitude according to the wavefront sensor residuals provided little improvement in the performance of the AO correction. Figure 7 shows the RMS residual phase across the pupil as a function of time during 8s simulations using a fixed modulation amplitude and using variable modulation amplitude. The mean level of RMS residual phase is shown in Table 1. However for the two intermittent turbulence models, varying the tip-tilt modulation amplitude did significantly reduce the RMS residual phase in the pupil, as can be seen in Figures 8 and 9 and in Table 1. It is clear that realistic simulation of turbulent intermittency will be essential when designing and testing real AO systems which respond actively to the seeing conditions.

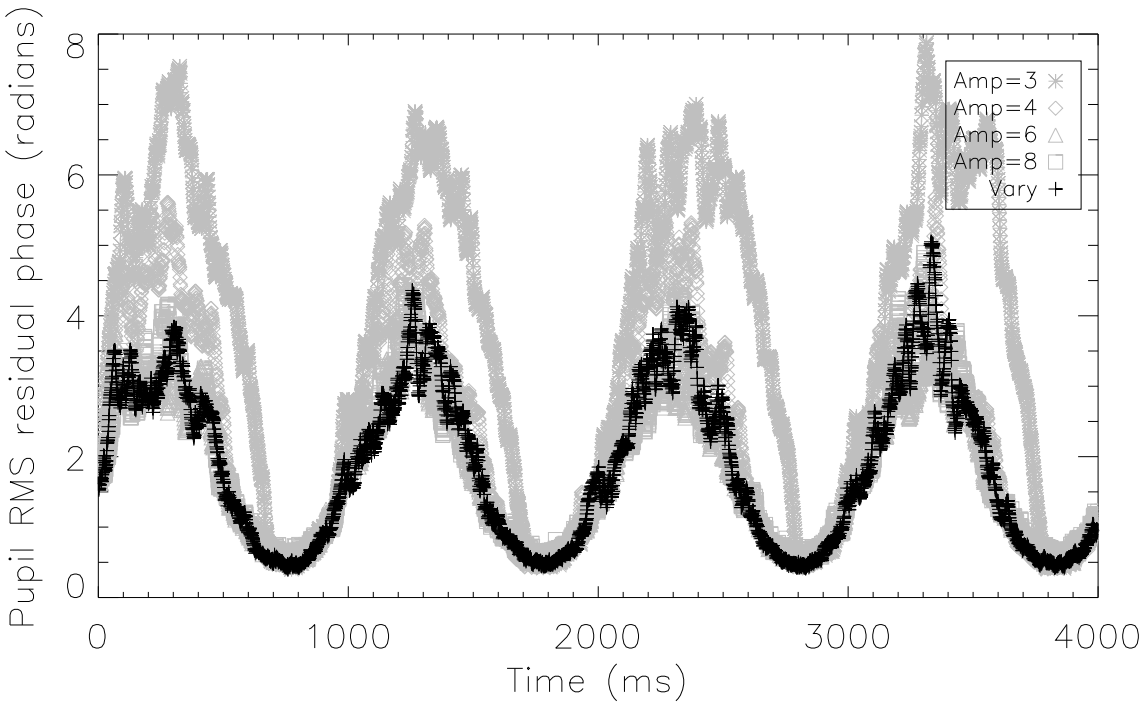

Figure 6. Assessing the optimum tip-tilt modulation amplitude for different turbulence strengths.

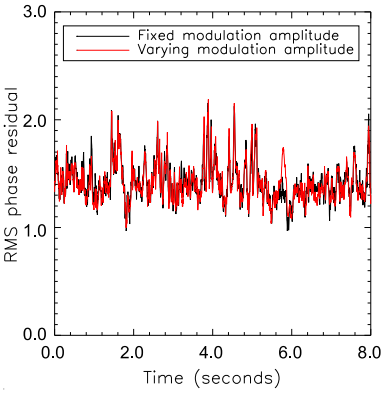

Figure 7. No turbulent intermittency.

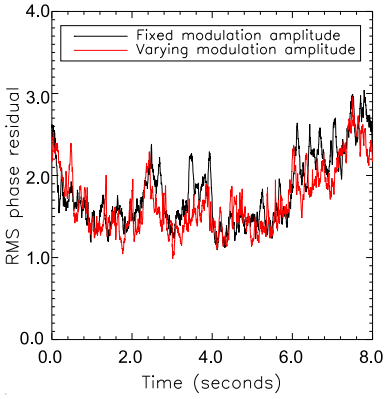

Figure 8. Normal distribution of turbulence strengths.

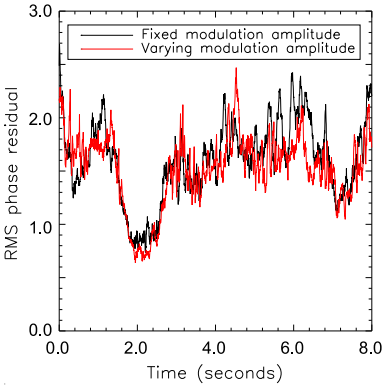

Figure 9. Log-Normal distribution of turbulence strengths.

	No intermittency	Normal distribution	Log Normal
Varying modulation	1.41	1.52	1.70
Fixed modulation	1.42	1.60	1.80

Table 1. RMS phase residual in the pupil after AO correction.

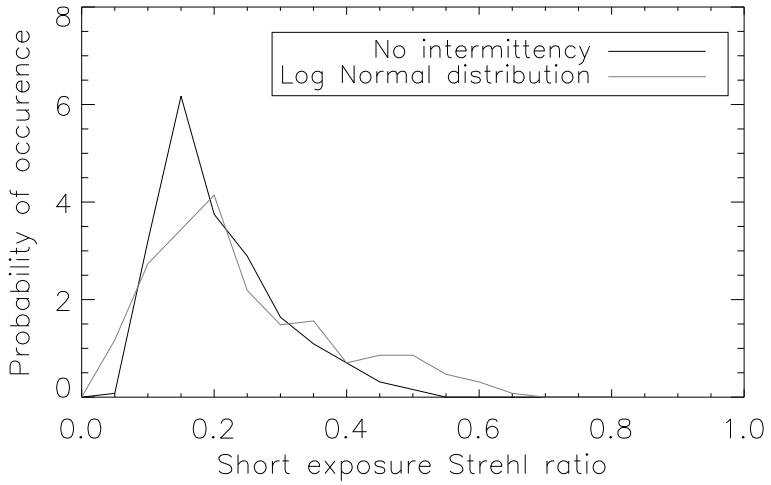

Figure 10. Effect of intermittency on short exposure Strehl ratios.

No turbulent intermittency	Log Normal distribution of turbulence strengths
0.384	0.506

Table 2. RMS variation in Strehl as a fraction of the mean Strehl ratio for each simulation.

7. EFFECT OF TURBULENT INTERMITTENCY ON LUCKY IMAGING

The LI method for high-resolution imaging relies on the exploitation of brief moments when the atmosphere provides above average image quality.[6,23–25] Simulations used to investigate the likely performance of LI have generally assumed constant seeing conditions.[24–26] If there is a variation in the astronomical seeing, then moments of extremely good image quality might become more likely. For this reason, the LI method might benefit from high levels of turbulent intermittency.

In order to assess the effect of turbulent intermittency on LI, two simulations were performed without AO correction using a telescope of diameter $D = 5r_0$, one having a log normal distribution of turbulent intermittency, and one without intermittency. The intermittent turbulence model had an RMS variation of 16% about the mean turbulence strength, and the turbulence strength had an exponentially decaying temporal autocorrelation function, decorrelated over a timescale of 0.5s. The wind speed in the simulations was $20r_0\text{s}^{-1}$, and a frame rate of 20Hz was used.

Figure 10 shows the Strehl histograms which resulted from 16s simulations using each of the models. The turbulent intermittency significantly broadens the Strehl histogram, providing a substantial increase in the number of exposures having the highest Strehl ratios. A comparison of the fractional width of the distributions is shown in Table 2.

The shift-and-add image generated from the best 10% of exposures has a Strehl ratio of 37% for the simulation without intermittency, but this increases to 50% for the simulation including intermittent turbulence.

In the simulation with intermittent seeing, the selected exposures are most likely to occur at times when the turbulence is weakest. At these moments the timescale for phase changes in the pupil is also expected to be at its slowest. To assess the impact this has on the speed at which the image is changing, the fractional change in Strehl ratio was calculated from each exposure to the next.

The calculated fractional change in Strehl ratio from one exposure to the next was found to be dependent on the value of the Strehl ratio. For the exposures with the highest 10% of Strehl ratios the fractional change

in Strehl ratio from one exposure to the next is significantly lower than the mean fractional change (where the mean incorporates all of the exposures). Experimental measurements have previously found that at times when the Strehl ratio is highest there are slower changes in the speckle pattern, which can allow the use of particularly long exposure times for the LI method.[23,25] The difference is particularly apparent in the simulation with intermittency, where exposure selection reduces the RMS fractional change in Strehl ratio between adjacent exposures from 12% to 2.8% (for the model without intermittency the equivalent change is from 13% to 3.7%). This highlights the fact that high Strehl ratios are generally associated with those periods having the largest r_0 and hence the longest temporal coherence times. For similar reasons it would be expected that the isoplanatic angle should be slightly larger for the exposures having the highest Strehl ratios.

8. CONCLUSIONS

A simulation method is presented which can generate atmospheric phase screens exhibiting turbulent intermittency (time-varying seeing), but retaining the structure function and power spectrum expected from Kolmogorov or Von Karman turbulence models. The spectrum of turbulence fluctuations can be chosen by the user, allowing a wide range of intermittency models to be simulated. The model naturally incorporates one or more wind velocities as well as the decorrelation of the wind-blown turbulence with time.

Simulations of AO correction under intermittent seeing are presented. The variation of AO control system parameters in response to changes in the RMS wavefront sensor signals is found to improve the performance of the AO correction when the astronomical seeing conditions are varying with time. Under fixed astronomical seeing conditions the use of time-varying control system parameters provides little benefit.

Simulations of Lucky Imaging (LI) show that this method provides higher image quality if the seeing conditions are time-varying, for a given mean turbulence strength. The coherence timescales for the exposures with the highest Strehl ratios is found to be higher in simulations having turbulent intermittency, and the isoplanatic angle is also expected to be higher for these exposures.

REFERENCES

1. G. K. Batchelor and A. A. Townsend, "The nature of turbulent motion at large wave-numbers," in *Proceedings of the Royal Society of London A, 199*, pp. 238–255, May 1949.
2. R. Racine, "Temporal Fluctuations of Atmospheric Seeing," *Proceedings of the Astronomical Society of the Pacific* **108**, pp. 372+, Apr. 1996.
3. M. S. Sarazin, "Automated seeing monitoring for queue-scheduled astronomical observations," in *Progagation and Imaging Through the Atmosphere*, L. R. Bossonnette and C. Dainty, eds., *Proc. SPIE* **3125**, pp. 366–+, 1997.
4. J. Vernin and C. Muñoz-Tuñón, "The temporal behaviour of seeing," *New Astronomy Review* **42**, pp. 451–454, Nov. 1998.
5. A. Tokovinin, S. Baumont, and J. Vasquez, "Statistics of turbulence profile at Cerro Tololo," *Monthly Notices of the Royal Astronomical Society* **340**, pp. 52–58, Mar. 2003.
6. N. M. Law, C. D. Mackay, and J. E. Baldwin, "Lucky imaging: high angular resolution imaging in the visible from the ground," *Astronomy and Astrophysics* **446**, pp. 739–745, Feb. 2006.
7. R. W. Wilson, "Personal communication – results from SLODAR measurements at Paranal and Roque de los Muchachos Observatory," Dec. 2005.
8. Y. Kim and D. L. Jaggard, "Band-limited fractal model of atmospheric refractivity fluctuation," *Optical Society of America Journal* **5**, pp. 475–480, Apr. 1988.
9. E. D. Siggia, "Model of intermittency in three-dimensional turbulence," *Physical Review A* **17**, pp. 1166–1176, Mar. 1978.
10. U. Frisch, P. Sulem, and M. Nelkin, "A simple dynamical model of intermittent fully developed turbulence," *Journal of Fluid Mechancis* **87**, pp. 719–736, 1978.
11. B. B. Mandelbrot, "Intermittent turbulence in self-similar cascades: divergence of high moments and dimension of the carrier," *Journal of Fluid Mechancis* **62**, pp. 331–358, 1974.
12. A. Y.-S. Kuo and S. Corrsin *Journal of Fluid Mechancis* **56**, p. 447, 1972.

13. V. I. Tatarski, *Wave Propagation in a Turbulent Medium*, McGraw-Hill, 1961.
14. A. Glindemann, R. G. Lane, and J. C. Dainty, "Simulation of Time-evolving Speckle Patterns Using Kolmogorov Statistics," *Journal of Modern Optics* **40**, pp. 2381–2388, Dec. 1993.
15. S. W. Smith, *The Scientist and Engineer's Guide to Digital Signal Processing*, California Technical Publishing, 1997.
16. D. Saint-Jacques, *Astronomical Seeing in Space and Time*. PhD thesis, Cambridge University, 1998.
17. D. Saint-Jacques and J. E. Baldwin, "Taylor's hypothesis: good for nuts," in *Interferometry in Optical Astronomy*, P. Lena and A. Quirrenbach, eds., *Proc. SPIE* **4006**, pp. 951–962, July 2000.
18. D. F. Buscher, J. T. Armstrong, C. A. Hummel, A. Quirrenbach, D. Mozurkewich, K. J. Johnston, C. S. Denison, M. M. Colavita, and M. Shao, "Interferometric seeing measurements on Mt. Wilson: power spectra and outer scales," *Applied Optics* **34**, pp. 1081–1096, Feb. 1995.
19. N. S. Nightingale and D. F. Buscher, "Interferometric seeing measurements at the La Palma Observatory," *Monthly Notices of the Royal Astronomical Society* **251**, pp. 155–166, July 1991.
20. J. W. O'Byrne, "Seeing measurements using a shearing interferometer," *Proceedings of the Astronomical Society of the Pacific* **100**, pp. 1169–1177, Sept. 1988.
21. M. M. Colavita, M. Shao, and D. H. Staelin, "Atmospheric phase measurements with the Mark III stellar interferometer," *Applied Optics* **26**, pp. 4106–4112, Oct. 1987.
22. M. Carbillet, A. Riccardi, and S. Esposito, "Numerical simulation studies for the first-light adaptive optics system of the Large Binocular Telescope," in *Advancements in Adaptive Optics*, B. L. Ellerbroek and R. Ragazzoni, eds., *Proc. SPIE* **5490**, pp. 721–732, Oct. 2004.
23. R. N. Tubbs, J. E. Baldwin, C. D. Mackay, and G. C. Cox, "Diffraction-limited CCD imaging with faint reference stars," *Astronomy and Astrophysics* **387**, pp. L21–L24, May 2002.
24. D. L. Fried, "Probability of getting a lucky short-exposure image through turbulence," *Optical Society of America Journal* **68**, pp. 1651–1658, Dec. 1978.
25. R. N. Tubbs, *Lucky Exposures: Diffraction limited astronomical imaging through the atmosphere*. PhD thesis, Cambridge University, Sept. 2003.
26. J. E. Baldwin, R. N. Tubbs, G. C. Cox, C. D. Mackay, R. W. Wilson, and M. I. Andersen, "Diffraction-limited 800 nm imaging with the 2.56 m Nordic Optical Telescope," *Astronomy and Astrophysics* **368**, pp. L1–L4, Mar. 2001.